

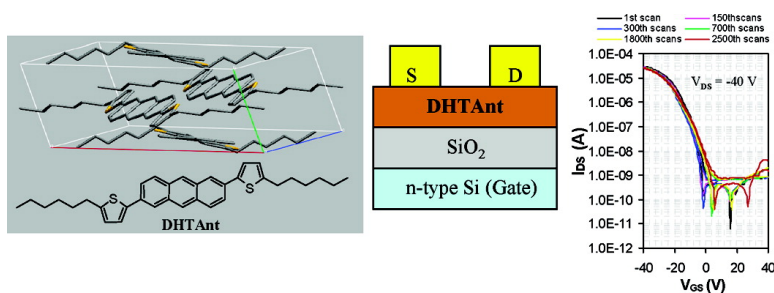
Communication

High-Performance, Stable Organic Thin-Film Field-Effect Transistors Based on Bis-5'-alkylthiophen-2'-yl-2,6-anthracene Semiconductors

Hong Meng, Fangping Sun, Marc B. Goldfinger, Gary D. Jaycox, Zhigang Li, Will J. Marshall, and Gregory S. Blackman

J. Am. Chem. Soc., **2005**, 127 (8), 2406-2407 • DOI: 10.1021/ja043189d • Publication Date (Web): 03 February 2005

Downloaded from <http://pubs.acs.org> on March 24, 2009



More About This Article

Additional resources and features associated with this article are available within the HTML version:

- Supporting Information
- Links to the 35 articles that cite this article, as of the time of this article download
- Access to high resolution figures
- Links to articles and content related to this article
- Copyright permission to reproduce figures and/or text from this article

[View the Full Text HTML](#)

High-Performance, Stable Organic Thin-Film Field-Effect Transistors Based on Bis-5'-alkylthiophen-2'-yl-2,6-anthracene Semiconductors

Hong Meng,* Fangping Sun, Marc B. Goldfinger, Gary D. Jaycox, Zhigang Li, Will J. Marshall, and Gregory S. Blackman

Central Research and Development, Experimental Station, E. I. DuPont Company, Wilmington, Delaware 19880-0328

Received November 11, 2004; E-mail: hong.meng@usa.dupont.com

The fabrication of flexible circuitry using modified printing technologies is emerging as a low cost product alternative to amorphous Si technology.¹ The key component of such circuitry is the organic thin-film transistor (OTFT). Although the field-effect mobility of OTFTs is still lower than those of the inorganic thin-film transistors, the advantages of easy manufacturing and processing make them suitable for selected commercial applications, such as electrophoretic displays.²

A critical technical challenge in this area of research is to improve the environmental stability of OTFTs.³ OTFTs have been fabricated incorporating semiconductors based on a wide variety of organic structure classes.⁴ The most promising performance has been observed for oligothiophene derivatives and linearly fused polycyclic aromatic compounds such as pentacene and its derivatives,^{5,6} yet the stability of these semiconductor types is limited.^{3b} Recent developments by several groups have resulted in improved stability, primarily through the judicious choice of conjugated units and side chains. However, the improved stability comes at the cost of lower field-effect mobilities and higher substrate deposition temperatures, the latter precluding application to plastic substrates.^{6a,b} Still needed are environmentally stable organic semiconductors with high mobility and on/off current ratios that can be deposited at low substrate temperatures.

In this communication, we report two novel semiconductors based on thiophene–anthracene oligomers that show field-effect mobilities as high as 0.50 cm²/Vs and on/off ratios greater than 10⁷. Most importantly, we have found that the stability of OTFTs fabricated with these materials is significantly improved relative to those measured for pentacene-based devices.^{3b} In addition, the high mobility of such semiconductors can be achieved at relatively low substrate deposition temperatures.

The semiconductors were synthesized using a Suzuki coupling reaction between pinacolato boronic ester-substituted 2,6-anthracene and the corresponding 2-bromothiophenes. UV–vis spectra of these semiconductors as deposited thin films showed a maximum wavelength absorption peak at 445 nm. This corresponds to an energy gap of 2.8 eV, significantly higher than that of pentacene (2.2 eV), possibly explaining the greater stability of these materials relative to that of pentacene.⁷ Both **DTAnt** and **DHTAnt** are soluble in hot toluene or xylene, which allows these semiconductors to be purified by a combination of recrystallization and gradient sublimation. The compounds were characterized by ¹H NMR, ¹³C NMR, high-resolution mass spectrometry, elemental analysis, and X-ray crystallography.

Figure 1 shows the molecular and crystallographic packing structures of the semiconductors **DTAnt** and **DHTAnt**. Both molecules display a nearly flat, symmetric molecular geometry, which facilitates tight molecular packing. The molecules pack in the herringbone geometry, similar to pentacene.⁷ The XRD reflec-

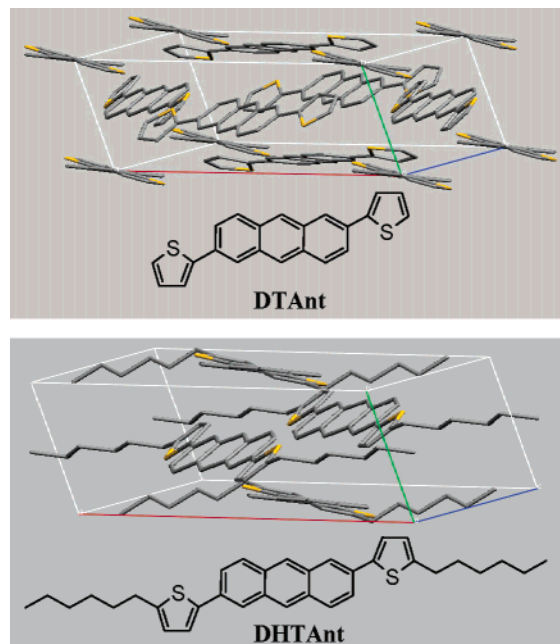


Figure 1. Crystal packing view of the unit cell of the semiconductors **DTAnt**: (*Pccn*, $a = 34.243(7)$ Å, $b = 7.5118(15)$ Å, $c = 6.0908(12)$ Å, $V = 1566.7(5)$ Å³, $Z = 4$) and **DHTAnt**: (*P21*, $a = 31.075(6)$ Å, $b = 7.3950(15)$ Å, $c = 5.8660(12)$ Å, $\beta = 93.97(3)^\circ$, $V = 1344.8(5)$ Å³, $Z = 4$).

tion patterns of the thin films of these materials suggest the same packing motifs as those observed in the single-crystal data and will be described in detail elsewhere.

OTFT devices were fabricated in a “top contact” geometry.⁸ Semiconductors were evaporated onto a SiO₂ (200 nm)/n-doped Si substrate. Gold was evaporated as the source/drain electrodes.

Table 1 lists the semiconductor OTFT device data deposited over a range of substrate temperatures. All OTFTs showed very well-defined linear- and saturation-regime output characteristics (see Supporting Information). Interestingly, the mobility of thiophene–anthracene **DTAnt** was 1 order of magnitude lower than that of the hexyl-substituted **DHTAnt**. This is likely due to the self-assembly properties of the alkyl side chain, which leads to more ordered films, especially at high substrate temperatures.⁹ This is in agreement with differential scanning calorimetry (DSC) measurements, which indicate that **DHTAnt** has high-temperature liquid crystalline mesophases, while **DTAnt** shows only a melt transition with no mesophase observed. Further increasing the substrate temperatures for **DHTAnt** decreases the device performance. A similar trend has been observed in pentacene and oligothiophenes.⁵

As corroborated by AFM measurements, the low mobility of the devices under high substrate deposition temperatures is due to

Table 1. OTFT Data (Average of Eight Individual Devices) of the Semiconductors under Different Substrate Deposition Temperatures

SC material	T_{sub} (°C)	μ (cm ² /Vs)	on/off	V_t (V)	SubTS (V/d)
DTAnt	23	0.037 ± 0.004	9.15 × 10 ⁵	−13.6	2.40
	60	0.048 ± 0.015	7.36 × 10 ⁶	−5.4	1.32
	80	0.063 ± 0.006	8.76 × 10 ⁵	−6.3	1.75
	90	0.035 ± 0.001	3.82 × 10 ⁵	−3.4	2.27
	100	0.025 ± 0.001	2.92 × 10 ⁵	−3.0	1.94
DHTAnt	20	0.13 ± 0.016	2.0 × 10 ⁶	−21.8	2.56
	60	0.31 ± 0.014	2.5 × 10 ⁷	−12.5	2.17
	80	0.34 ± 0.011	6.6 × 10 ⁸	−13.6	2.56
	100	0.48 ± 0.096	5.5 × 10 ⁷	−10.7	2.46
	120	0.21 ± 0.023	2.6 × 10 ⁷	−11.4	2.77
120/80	0.50 ± 0.045	2.8 × 10 ⁷	−10.4	1.87	

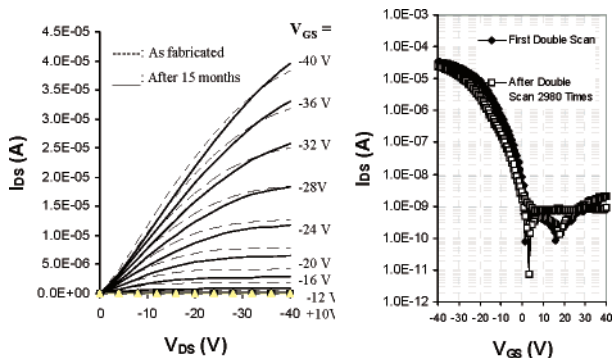


Figure 2. Characteristics of DHTAnt OFET devices ($L = 60 \mu\text{m}$, $W = 600 \mu\text{m}$) fabricated at $T_{\text{sub}} 80 \text{ }^\circ\text{C}$. (Left) Plot of I_{DS} vs V_{GS} at various gate voltages: Shelf life time test. (Right) Plots of I_{DS} vs V_{GS} at constant $V_{\text{DS}} = -40 \text{ V}$: Operation-lifetime test. (NB: Current data are absolute values.)

voids or cracks formed under elevated substrate temperature. The origin of the cracks is likely due to different thermal expansion coefficients between the semiconductor and the substrate. To further investigate these morphology issues, we fabricated FETs using a multiple-deposition method.¹⁰ By first evaporating to a 20-nm-thickness film under a high substrate deposition temperature (120 °C), we were able to cover the majority of the surface, maintaining the large grain size of the semiconductor. The cracks and voids were then filled during a second 20-nm deposition at a lower substrate deposition temperature (80 °C). By depositing the semiconductor using this two-stage process, we were able to increase the device mobility to 0.50 cm²/Vs with an on/off current ratio of 10⁷.

To test the device stability, we performed both shelf life tests and continuous operation tests under ambient conditions. In the shelf life test, the device mobility and on/off ratios were measured periodically over a span of 15 months. Figure 2 (left) shows the I_V characteristics of the device before and after 15 months of storage, over which time the performance of the device was largely unchanged. The mobility varied from 0.35 to 0.42 cm²/Vs, and the on/off ratio varied from 1.1×10^6 to 4.7×10^7 . In the operation-lifetime tests, the device was subjected to continuous operation under a constant drain–source voltage V_{DS} of -40 V and a continuous sweeping of gate–source voltages V_{GS} between $+40$ and -40 V . Figure 2 (right) plots the characteristics of I_{DS} versus V_{GS} during the first gate voltage scan (double scan done in forward and reverse bias) between $+40$ and -40 V and after approximately 2960 double scans, showing little drop in performance. In all cases there is no obvious hysteresis present in the I_V curves. DTAnt-based OTFT exhibited similar stability as DHTAnt.

We also fabricated OTFTs using these semiconductors on plastic substrates with organic dielectric materials as insulators. Their performance was the same as that with the silicon wafer substrates, and these results will be reported elsewhere.

In conclusion, we have synthesized two novel organic semiconductors based on thiophene–anthracene molecules, which show remarkably high stability and very good electrical characteristics, rendering these materials excellent OTFT semiconductors for flexible electronics applications.

Acknowledgment. We thank our colleagues I. Malajovich, R. J. Chesterfield, J. S. Meth, F. Gao, G. Nunes, L. K. Johnson, H. E. Simmons, C. R. Fincher, G. B. Blanchet, P. F. Garcia, K. G. Sharp, and K. L. Adams for useful discussions. We are grateful to K. D. Dobbs for molecular modeling; R. S. McLean and D. J. Brill for AFM; E. Y. Hung and C. M. Ruley for MS; S. A. Hill for NMR; D. J. Redmond and R. V. Davidson for XRD; and R. A. Twaddell, M. Y. Keating, and S. Ahoorai for TGA and DSC tests. H.M. thanks Prof. Bao and Prof. Perepichka for valuable discussions.

Supporting Information Available: Details of experimental procedures and additional data or spectra, information of OTFT device fabrication (PDF), and X-ray crystal structure (CIF). This material is available free of charge via the Internet at <http://pubs.acs.org>.

References

- (1) (a) Horowitz, G. *J. Mater. Res.* **2004**, *19*, 1946. (b) Kelley, T. W.; Baude, P. F.; Gerlach, C.; Ender, D. E.; Muires, D.; Haase, M. A.; Vogel, D. E.; Theiss, S. D. *Chem. Mater.* **2004**, *16*, 4413. (c) Dimitrakopoulos, C. D.; Malenfant, P. R. L. *Adv. Mater.* **2002**, *14*, 99. (d) Bao, Z. *Adv. Mater.* **2000**, *12*, 227.
- (2) (a) Baude, P. F.; Ender, D. A.; Haase, M. A.; Kelley, T. W.; Muires, D. V.; Theiss, S. D. *Appl. Phys. Lett.* **2003**, *82*, 3964. (b) Blanchet, G. B.; Loo, Y.; Rogers, J. A.; Gao, F.; Fincher, C. R. *Appl. Phys. Lett.* **2003**, *82*, 463. (c) Gelinck, G. H.; Huitema, H. E. A.; van Veenendaal, E.; Cantatore, E.; Schrijnemakers, L.; van der Putten, J. B. P. H.; Geuns, T. C. T.; Beenhakkers, M.; Giesbers, J. B.; Huisman, B.; Meijer, E. J.; Benito, E. M.; Touwslager, F. J.; Marsman, A. W.; van Rens, B. J. E.; de Leeuw, D. M. *Nat. Mater.* **2004**, *3*, 106.
- (3) (a) Qiu, Y.; Hu, Y.; Dong, G.; Wang, L.; Xie, J.; Ma, Y. *Appl. Phys. Lett.* **2003**, *83*, 1644. (b) Pannemann, Ch.; Diekmann, T.; Hilleringmann, U. *J. Mater. Res.* **2004**, *19*, 1999.
- (4) (a) Gorjanc, T. C.; Levesque, I.; D'Orio, M. *Appl. Phys. Lett.* **2004**, *84*, 930. (b) Katz, H. E. *Chem. Mater.* **2004**, *16*, 4748.
- (5) (a) Facchetti, A.; Musherush, M.; Yoon, M.; Hutchison, G. R.; Ratner, M. A.; Marks, T. J. *J. Am. Chem. Soc.* **2004**, *126*, 13859. (b) Murphy, A. R.; Frechet, J. M. J.; Chang, P.; Lee, J.; Subramanian, V. *J. Am. Chem. Soc.* **2004**, *126*, 1596. (c) Mas-Torrent, M.; Durkut, M.; Hadley, P.; Ribas, X.; Rovira, C. *J. Am. Chem. Soc.* **2004**, *126*, 984. (d) Lin, Y.-Y.; Gundlach, D. J.; Nelson, S. F.; Jackson, T. N. *IEEE Trans. Electron Devices* **1997**, *44*, 1325. (e) Sakamoto, Y.; Suzuki, T.; Kobayashi, M.; Gao, Y.; Fukai, Y.; Inoue, Y.; Sato, F.; Tokito, S. *J. Am. Chem. Soc.* **2004**, *126*, 8138. (f) Meng, H.; Bendikov, M.; Mitchell, G.; Helgeson, R.; Wudl, F.; Bao, Z.; Siegrist, T.; Kloc, C.; Chen, C. *Adv. Mater.* **2003**, *15*, 1090. (g) Sheraw, C. D.; Jackson, T. N.; Eaton, D. L.; Anthony, J. E. *Adv. Mater.* **2003**, *15*, 2009.
- (6) (a) Ito, K.; Suzuki, T.; Sakamoto, Y.; Kubota, D.; Inoue, Y.; Sato, F.; Tokito, S. *Angew. Chem., Int. Ed.* **2003**, *42*, 1159. (b) Meng, H.; Zheng, J.; Lovinger, A. J.; Wang, B.; Van Patten, P. G.; Bao, Z. *Chem. Mater.* **2003**, *15*, 1778. (c) Miao, Q.; Nguyen, T.; Someya, T.; Blanchet, G. B.; Nuckolls, C. *J. Am. Chem. Soc.* **2003**, *125*, 10284. (d) Musherush, M.; Facchetti, A.; Lefenfeld, M.; Katz, H. E.; Marks, T. J. *J. Am. Chem. Soc.* **2003**, *125*, 9414. (e) Laquindanum, J. G.; Katz, H. E.; Lovinger, A. J. *J. Am. Chem. Soc.* **1998**, *120*, 664.
- (7) (a) Cornil, J.; Calbert, J. Ph.; Bredas, J. L. *J. Am. Chem. Soc.* **2001**, *123*, 1250. (b) Fritz, S. E.; Martin, S. M.; Frisbie, C. D.; Ward, M. D.; Toney, M. F. *J. Am. Chem. Soc.* **2004**, *126*, 4084.
- (8) Horowitz, G. *Adv. Mater.* **1998**, *10*, 365.
- (9) Garnier, F.; Yassar, A.; Hajlaoui, R.; Horowitz, G.; Deloffre, F.; Servet, B.; Ries, S.; Alnot, P. *J. Am. Chem. Soc.* **1993**, *115*, 8716.
- (10) (a) Lin, Y. Y.; Gundlach, D. J.; Nelson, S. F.; Jackson, T. N. *IEEE Electron Device Lett.* **1997**, *18*, 606. (b) Horowitz, G.; Hajlaoui, M. E. *Adv. Mater.* **2000**, *12*, 1046.

JA043189D